Journal of Sound and Vibration (1998) **210**(5), 581–592

NEW ADMISSIBLE FUNCTIONS FOR THE DYNAMIC ANALYSIS OF A SLEWING FLEXIBLE BEAM

M. K. KWAK

Department of Mechanical Engineering, Dongguk University, 26 Pil-Dong 3-Ga, Joong-Gu, Seoul 100-715, Korea

(*Received 29 April 1997, and in final form 15 September 1997*)

An important question associated with the modelling of a slewing beam is the discretization of a continuous elastic beam. If discretization is performed by the assumed mode method, the question arises about the type of admissible functions to be used in series expansions. In this regard, the eigenfunctions of a non-rotating clamped–free uniform beam known as cantilever modes have been widely used as admissible functions for the dynamic analysis of the slewing beam. The discretization will be sufficient provided that the set of admissible functions is complete and a sufficiently large number of functions is used. However, there are cases that we need to approximate the model with a small number of admissible functions. Examples are numerical simulation and control design. In this paper, new admissible functions which approximate the dynamic characteristics of the slewing beam more accurately than the eigenfunctions of the non-rotating clamped–free uniform beam is developed and its efficiency is verified by numerical examples.

1. INTRODUCTION

A problem of current interest is the dynamic characteristics of a flexible beam undergoing large slewing motion. In order to describe the motion of the slewing flexible beam, a suitable reference frame needs to be chosen. In general, the motion of the slewing beam can be described by the rotation of a given reference frame and the elastic displacement relative to that frame, where the reference frame is often chosen so as to satisfy the zero slope at the root. The associated mathematical formulation is in terms of both ordinary and partial differential equations, resulting in the hybrid equations of motion. Here, the case in which the beam undergoes small elastic displacements relative to the reference frame attached to the rotating body axis, and the beam is rotated by the torque applied at the root of the beam is examined.

A common procedure for analyzing hybrid systems is discretization, whereby the partial differential equations are replaced by ordinary ones. There are many discretization procedures in common use, such as the Rayleigh–Ritz method, the finite element method, etc. The Rayleigh–Ritz method consists of expanding the displacement of a continuous elastic member in a finite series of known space-dependent functions multiplied by time-dependent generalized co-ordinates. Since the space-dependent functions used in such expansions generally represent vibration modes of a closely related system, the Rayleigh–Ritz method is often referred to as the assumed mode method [1].

The assumed mode method has been used extensively to obtain estimates of natural frequencies and modes of vibration of distributed-parameter systems including the gyroscopic system [1, 2]. In particular, Meirovitch [2] proved that stationary property exists for gyroscopic systems and showed that the system dynamic characteristics are not

0022–460X/98/100581 + 12 $25.00/0/sv971354

significantly affected by the type of functions used, provided that the set of functions is complete and a sufficiently large number of functions is used. If discretization is performed by the assumed mode method in the case of the slewing flexible beam, the admissible functions to be used in series expansions should be chosen *a priori*. The eigenfunctions of the non-rotating clamped–free uniform beam have been widely used as assumed modes for the dynamic analysis of flexible multibody systems [3] and a slewing beam [4]. Garcia and Inman [5] studied the effect of servo stiffness on the dynamic analysis of a single-link flexible beam and concluded that the clamped–free beam assumption for the dynamic analysis of the slewing beam is a valid assumption if the ratio of the servo stiffness to beam flexibility is high. Note that the eigenfunctions of the non-rotating clamped–free uniform beam are in fact comparison functions since they satisfy both geometric and natural boundary conditions. However, there have been cases where severe truncation is involved. The modelling accuracy becomes a great concern when simulating the motion of a slewing beam and designing controls for such a system. In other words, the model obtained by the assumed mode method should contain minimal error in representing the system with a small number of admissible functions. This motivated the author to pursue a new set of admissible functions for the dynamic analysis of the slewing beam.

If the slewing angle and elastic motions are small, the problem can be reduced to the case of a pinned–free beam based on an inertial frame. In this case, elastic displacements are expressed in terms of inertial co-ordinates. For instance, a single-link flexible beam under slewing motion where the pinned-end is actively controlled and the other end is free can be described either by the pinned–free beam based on inertial frame or the clamped–free beam based on the rotating body axis, provided that both the rigid-body motion and the elastic motion are small. This paper is concerned with the discretization of elastic motion of a beam undergoing large slewing motion. Thus, the rotating body axis is chosen as a reference frame and the elastic motion is described relative to the body axis. Although the eigenfunctions of the non-rotating clamped–free beam, so called cantilever modes, have been widely used as admissible functions for this case, it has been observed that resulting coefficient matrices are not suitable for numerical simulation and control design, since those coefficient matrices are stiff in nature. A new set of admissible functions was thus pursued, which leads to numerically stable coefficient matrices.

The new set of admissible functions were obtained in reference [6] by solving the linearized hybrid equation of motion for a rotationally accelerated uniform beam. However, the validity of new admissible functions was not checked for the numerical computation. In this paper, the discretized equations of motion are presented and the numercial results by new admissible functions are compared to the results obtained by the cantilever modes. As a result, accurate natural frequencies and modes are obtained in lower modes by both assumed modes. However, higher modes suffer in the case of eigenfunctions of the non-rotating clamped–free uniform beam. Both assumed modes are applied to the dynamic simulation of the slewing beam. Numerical results show that eigenfunctions of the non-rotating clamped–free uniform beam suffer in simulating responses of the slewing beam since it does not realize higher modes. On the other hand, the new admissible functions developed give stable simulation results.

2. MODELLING OF A SLEWING NON-UNIFORM BEAM

Consider a non-uniform beam moving on a horiziontal surface (Figure 1). The beam is assumed to be thin compared to its length. The interest lies in deriving equations of

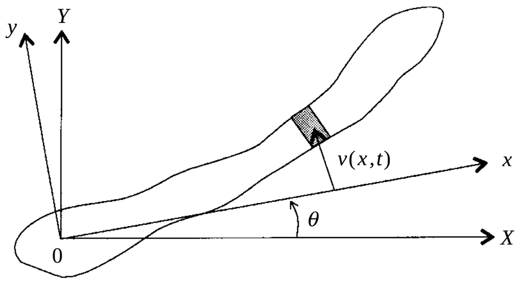

Figure 1. A slewing beam.

motion. To formulate the problem, the extended Hamilton principle given by

$$\int_{t_1}^{t_2} (\partial T + \partial W)\,\mathrm{d}t = 0 \tag{1}$$

is used, where T is the kinetic energy and W is the total work consisting of the conservative and non-conservative works. To this end, the velocity expression at a nominal point in the beam needs to be derived. The position vector of a nominal point in the beam with respect to the inertial co-ordinates can be expressed as

$$\mathbf{R}_p = \hat{\mathbf{n}}^T C^T(\boldsymbol{\xi} + \mathbf{u}), \tag{2}$$

where $\mathbf{R}_p = R_{px}\mathbf{I} + R_{py}\mathbf{J}$ represents the position vector of the point of interest and

$$\hat{\mathbf{n}} = \begin{bmatrix} \mathbf{I} \\ \mathbf{J} \end{bmatrix}, \qquad \boldsymbol{\xi} = \begin{bmatrix} x \\ 0 \end{bmatrix}, \qquad \mathbf{u} = \begin{bmatrix} 0 \\ v \end{bmatrix}, \qquad C = C(\theta) = \begin{bmatrix} \cos\theta & \sin\theta \\ -\sin\theta & \cos\theta \end{bmatrix}, \tag{3}$$

in which $\hat{\mathbf{n}}$ is the unit vector for inertial co-ordinates, and C is the matrix of the direction cosines between the xy and XY axes. The velocity vector can then be derived by taking the time-derivative of equation (2):

$$\dot{\mathbf{R}}_p = \hat{\mathbf{n}}^T[\dot{C}^T(\boldsymbol{\xi} + \mathbf{u}) + C^T\dot{\mathbf{u}}] = \hat{\mathbf{n}}^T[-\dot{\theta}D^T(\boldsymbol{\xi} + \mathbf{u}) + C^T\dot{\mathbf{u}}] = \hat{\mathbf{n}}^T\mathbf{V}_p, \tag{4}$$

where

$$D = D(\theta) = \begin{bmatrix} \sin\theta & -\cos\theta \\ \cos\theta & \sin\theta \end{bmatrix}. \tag{5}$$

To obtain the kinetic energy, the velocity squared needs to be computed. Hence, one obtains

$$\begin{aligned} v_p^2 &= \dot{\mathbf{R}}_p \cdot \dot{\mathbf{R}}_p = \mathbf{V}_p^T\mathbf{V}_p \\ &= \dot{\theta}^2(\boldsymbol{\xi} + \mathbf{u})^T(\boldsymbol{\xi} + \mathbf{u}) - 2\dot{\theta}(\boldsymbol{\xi} + \mathbf{u})^T DC^T\dot{\mathbf{u}} + \dot{\mathbf{u}}^T\dot{\mathbf{u}}. \end{aligned} \tag{6}$$

Recalling equations (3) and using the relation,

$$DC^T = \begin{bmatrix} 0 & -1 \\ 1 & 0 \end{bmatrix}, \tag{7}$$

TABLE 1

βL for uniform beam

	Clamped–free	Pinned–free
1	1·87510407	3·92660231
2	4·69409113	7·06858275
3	7·85475744	10·21017612
4	10·99554073	13·35176878
5	14·13716839	16·49336143
$i \geqslant 6$	$(2i-2)\pi/2$	$(4i+2)\pi/4$

equation (6) can be rewritten

$$v_p^2 = x^2\dot{\theta}^2 + \dot{\theta}^2 v^2 + 2x\dot{\theta}\dot{v} + \dot{v}^2. \tag{8}$$

Thus, using equation (8), the kinetic energy can be derived

$$T = \tfrac{1}{2}\int_0^L \bar{m}v_p^2\,\mathrm{d}x = \tfrac{1}{2}J\dot{\theta}^2 + \tfrac{1}{2}\dot{\theta}^2\int_0^L \bar{m}v^2\,\mathrm{d}x + \dot{\theta}\int_0^L \bar{m}\dot{v}^2\,\mathrm{d}x + \tfrac{1}{2}\int_0^L \bar{m}\dot{v}^2\,\mathrm{d}x, \tag{9}$$

where L is the length of the beam, $\bar{m}$ represents the mass per unit length, and $J = \int_0^L \bar{m}x^2\,\mathrm{d}x$ represents the mass moment of inertia with respect to the hinge point.

Potential energy can be expressed as

$$V = [v, v] = \tfrac{1}{2}\int_0^L EI\left(\frac{\partial^2 v}{\partial x^2}\right)^2 \mathrm{d}x, \tag{10}$$

and the virtual work is

$$\delta W = -\delta V + \tau\delta\theta \tag{11}$$

where τ is the torque applied to the hub of the beam.

Inserting equations (9) and (11) into equation (1) and considering that the virtual displacements, $\delta\theta$ and δv, are arbitrary and independent, one has

$$J\ddot{\theta} + \ddot{\theta}\int_0^L \bar{m}v^2\,\mathrm{d}x + 2\dot{\theta}\int_0^L \bar{m}v\dot{v}\,\mathrm{d}x + \int_0^L \bar{m}x\ddot{v}\,\mathrm{d}x = \tau, \tag{12}$$

$$\bar{m}(\ddot{v} + x\ddot{\theta} - \dot{\theta}^2 v) + EI\frac{\partial^4 v}{\partial x^4} = 0, \qquad 0 < x < L, \tag{13}$$

and boundary conditions

$$v(0) = \left.\frac{\partial v}{\partial x}\right|_{x=0} = \left.EI\frac{\partial^2 v}{\partial x^2}\right|_{x=L} = \left.EI\frac{\partial^3 v}{\partial x^3}\right|_{x=L} = 0. \tag{14}$$

3. EIGENVALUE PROBLEM FOR A SLEWING UNIFORM BEAM

The linearized version of equations (12) and (13) can be written as

$$J\ddot{\theta} + \int_0^L \bar{m}x\ddot{v}\,\mathrm{d}x = \tau, \tag{15}$$

$$\bar{m}(\ddot{v} + x\ddot{\theta}) + EI\frac{\partial^4 v}{\partial x^4} = 0, \qquad 0 < x < L. \tag{16}$$

Consider the free vibration of a slewing uniform beam. Using equations (15) and (16), one can obtain

$$\ddot{\theta} = -\frac{3}{L^3}\int_0^L x\ddot{v}\,\mathrm{d}x, \tag{17}$$

$$\bar{m}\ddot{v} + EI\frac{\partial^4 v}{\partial x^4} = -\bar{m}x\ddot{\theta}, \qquad 0 < x < L. \tag{18}$$

Inserting equation (17) into equation (18), one obtains

$$\bar{m}\ddot{v} + EI\frac{\partial^4 v}{\partial x^4} = \frac{3\bar{m}x}{L^3}\int_0^L \xi\ddot{v}\,\mathrm{d}\xi. \tag{19}$$

Introducing $v(x, t) = V(x)\,\mathrm{e}^{i\omega t}$ into the above equation yields

$$EI\frac{\mathrm{d}^4 V}{\mathrm{d}x^4} - \omega^2\bar{m}V = -\frac{\omega^2\bar{m}x}{L^3}\,x\int_0^L \xi V\,\mathrm{d}\xi. \tag{20}$$

The solution of equation (20) can be written as

$$V(x) = A\cosh(\beta x) + B\sinh(\beta x) + C\cos(\beta x) + D\sin(\beta x) + Ex. \tag{21}$$

Inserting equation (21) into equation (20), one obtains the following relation

$$E = \frac{3}{L^3}\int_0^L \xi V\,\mathrm{d}\xi, \tag{22}$$

which yields

$$A(\beta L\sinh\beta L - \cosh\beta L + 1) + B(\beta L\cosh\beta L - \sinh\beta L) + C(\beta L\sin\beta L + \cos\beta L - 1) + D(-\beta L\cos\beta L + \sin\beta L) = 0. \tag{23}$$

Inserting equation (21) into the boundary conditions, equations (14) result in

$$A + C = 0, \tag{24}$$

$$\beta(B + D) + E = 0, \tag{25}$$

$$A\cosh\beta L + B\sinh\beta L - C\cos\beta L - D\sin\beta L = 0, \tag{26}$$

$$A\sinh\beta L + B\cosh\beta L + C\sin\beta L - D\cos\beta L = 0. \tag{27}$$

Using equation (23) and equations (24–27), the characteristic equation can be obtained

$$\tanh \beta L = \tan \beta L, \tag{28}$$

and the mode shape can be expressed as

$$V(x) = \sin \beta x + \frac{\sin \beta L}{\sinh \beta L} \sinh \beta x - \beta\left(1 + \frac{\sin \beta L}{\sinh \beta L}\right)x. \tag{29}$$

It can be readily recognized that equation (28) is in fact the characteristic equation for a pinned–free beam, and equation (29) consists of the mode shape of a pinned–free beam and the linear equation whose constant is equal to the minus of the slope of the mode shape of a pinned–free beam at the root.

It is evident that the problem amounts to the eigenvalue problem of the pinned–free beam in the inertial frame.

4. SPATIAL DISCRETIZATION

Coupled integro–differential equations (15) and (16) do not permit an exact solution easily for a non-uniform beam. Thus, an approximate solution should be pursued by introducing admissible functions. This issue becomes more critical when designing controls since the control design for the hybrid equation is not feasible. The elastic displacement is discretized by introducing the admissible functions

$$v = v(x, t) = \sum_{j=1}^{n} \phi_j(x) q_j(t) = \mathbf{\Phi q}, \tag{30}$$

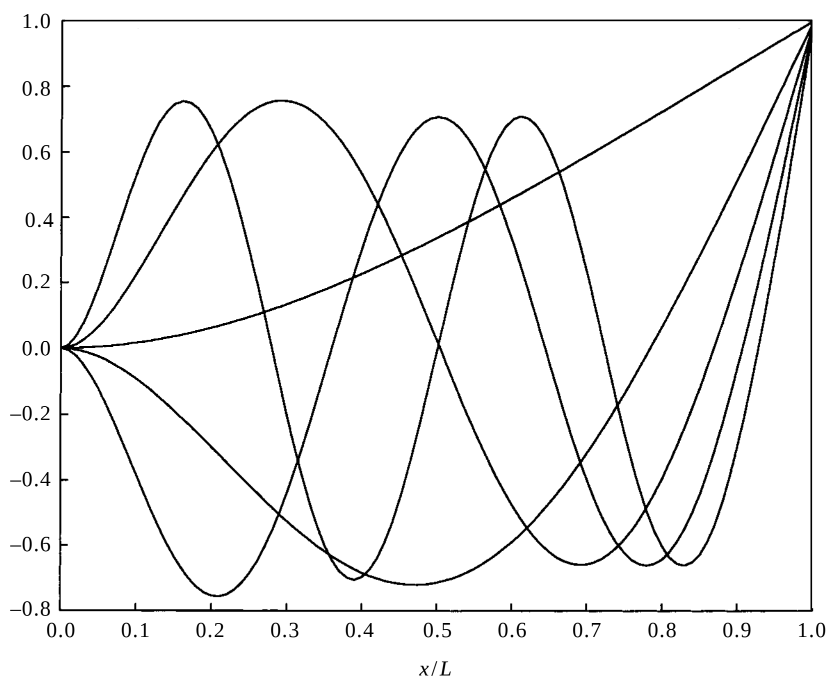

Figure 2. Clamped–free natural mode.

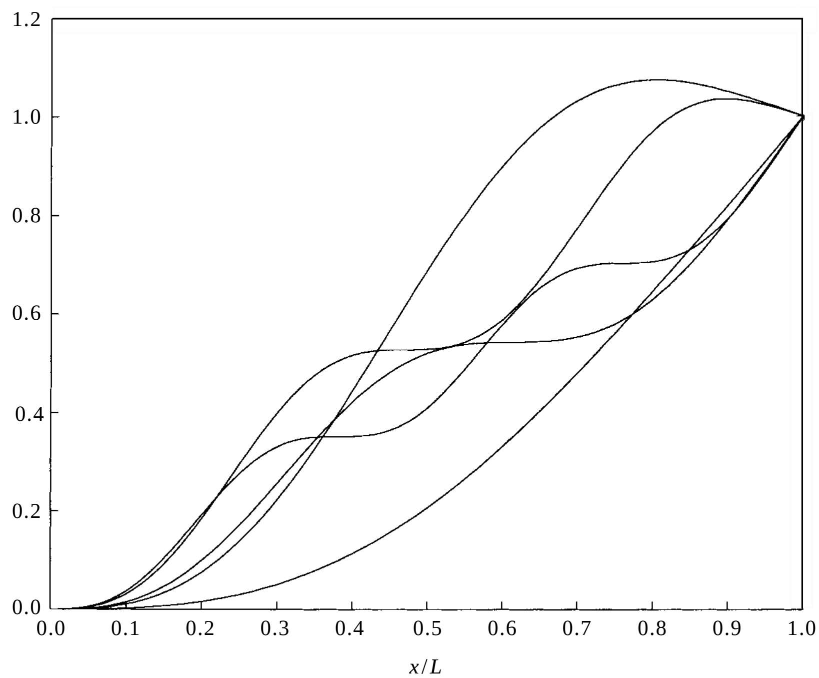

Figure 3. New admissible functions.

where

$$\mathbf{\Phi} = [\phi_1 \phi_2 \ldots \phi_n], \qquad \mathbf{q} = [q_1 q_2 \ldots q_n]^T, \tag{31}$$

in which ϕ_i and q_i $(i = 1, 2, \ldots)$ are admissible functions and generalized co-ordinates, respectively. The admissible functions introduced in the above equation should satisfy at least the geometric boundary conditions. If equation (30) is inserted into the kinetic energy, equation (9) results in

$$T = \tfrac{1}{2}J\dot{\theta}^2 + \tfrac{1}{2}\dot{\theta}^2\mathbf{q}^T + \dot{\theta}\tilde{\mathbf{\Phi}}\dot{\mathbf{q}} + \tfrac{1}{2}\dot{\mathbf{q}}^T M_e \dot{\mathbf{q}}, \tag{32}$$

where

$$M_e = \int_0^L \bar{m}\mathbf{\Phi}^T\mathbf{\Phi}\,\mathrm{d}x, \qquad \tilde{\mathbf{\Phi}} = \int_0^L \bar{m}x\mathbf{\Phi}\,\mathrm{d}x, \tag{33}$$

TABLE 2

The first natural frequency (Hz)

No. of modes	Clamped–free mode	New admissible function
1	3·854694	2·927607
2	2·930974	2·927560
3	2·928103	2·927343
4	2·927335	2·927314
5	2·927334	2·927301

TABLE 3

The second natural frequency (Hz)

No. of modes	Clamped–free mode	New admissible function
2	12·951840	8·762541
3	8·786614	8·762273
4	8·769150	8·760751
5	8·760906	8·760392

and the potential energy can be expressed as

$$V = \tfrac{1}{2}\mathbf{q}^T K_e \mathbf{q}, \tag{34}$$

where

$$K_e = \int_0^L EI \frac{\mathrm{d}^2\mathbf{\Phi}^T}{\mathrm{d}x^2}\frac{\mathrm{d}^2\mathbf{\Phi}}{\mathrm{d}x^2}\,\mathrm{d}x. \tag{35}$$

Thus, the virtual work can be expressed as

$$\partial W = -\delta\mathbf{q}^T K_e \mathbf{q} + \tau\delta\theta. \tag{36}$$

Inserting equations (32) and (36) into equation (1), and considering that the virtual displacements, $\delta\theta$ and $\delta\mathbf{q}$, are arbitrary and independent, one must have

$$J\ddot{\theta} + \ddot{\theta}\mathbf{q}^T M_e \mathbf{q} + 2\dot{\theta}\mathbf{q}^T M_e \dot{\mathbf{q}} + \tilde{\mathbf{\Phi}}\ddot{\mathbf{q}} = \tau, \tag{37}$$

$$\tilde{\mathbf{\Phi}}^T\ddot{\theta} + M_e\ddot{\mathbf{q}} + (K_e - \dot{\theta}^2 M_e)\mathbf{q} = 0. \tag{38}$$

A linearized version of the above equations can be written as

$$J\ddot{\theta} + \tilde{\mathbf{\Phi}}\ddot{\mathbf{q}} = \tau, \tag{39}$$

$$\tilde{\mathbf{\Phi}}^T\ddot{\theta} + M_e\ddot{\mathbf{q}} + K_e\mathbf{q} = 0. \tag{40}$$

Combining equations (39) and (40), one can write the matrix equations of motion

$$M\ddot{\mathbf{x}} + K\mathbf{x} = b\tau, \tag{41}$$

where $\mathbf{x} = [\theta \quad \mathbf{q}^T]^T$ and

$$M = \begin{bmatrix} J & \tilde{\mathbf{\Phi}} \\ \tilde{\mathbf{\Phi}}^T & M_e \end{bmatrix}, \qquad K = \begin{bmatrix} 0 & 0 \\ 0 & K_e \end{bmatrix}, \qquad b = \begin{bmatrix} 1 \\ 0 \end{bmatrix}. \tag{42}$$

In state form expression, we have

$$\dot{\mathbf{z}} = A\mathbf{z} + B\tau, \tag{43}$$

where $\mathbf{z} = [\mathbf{x}^T \ \dot{\mathbf{x}}^T]^T$ and

$$A = \begin{bmatrix} 0 & I \\ -M^{-1}K & 0 \end{bmatrix}, \qquad B = \begin{bmatrix} 0 \\ M^{-1}b \end{bmatrix}. \tag{44}$$

5. NUMERICAL EXAMPLE

Consider two candidates as an admissible function for a slewing non-uniform beam. The first one is the eigenfunction of a clamped–free beam:

$$\phi_i^{cf} = \sin\beta_i x - \sinh\beta_i x - \frac{\sin\beta_i L + \sinh\beta_i L}{\cos\beta_i L + \cosh\beta_i L}(\cosh\beta_i x - \cos\beta_i x), \qquad i = 1, 2, \ldots, \tag{45}$$

and the second one consists of the new admissible functions obtained by equation (29)

$$\phi_i^{new} = \sigma_i\left[\sin\beta_i x + \frac{\sin\beta_i L}{\sinh\beta_i L}\sinh\beta_i x - \beta_i\left(1 + \frac{\sin\beta_i L}{\sinh\beta_i L}\right)x\right], \qquad i = 1, 2, \ldots, \tag{46}$$

where

$$\sigma_i = \frac{1}{2\sin\beta_i L - \beta_i L(1 + (\sin\beta_i L/\sinh\beta_i L))}, \qquad i = 1, 2, \ldots, \tag{47}$$

in which σ_i is introduced to make the end displacement unity. The $\beta_i L$ for each mode shape is tabulated in Table 1 and its mode shapes are shown in Figures 2 and 3.

As a numerical example, the non-uniform beam which has the following property is considered.

$$\bar{m} = 1 - \frac{5}{6}\left(\frac{x}{L}\right)^3, \qquad EI = 1 - \frac{5}{6}\left(\frac{x}{L}\right)^3. \tag{48}$$

The first and second natural frequencies obtained by each admissible function are tabulated in Tables 2 and 3. As can be seen from these tables, the convergence in natural

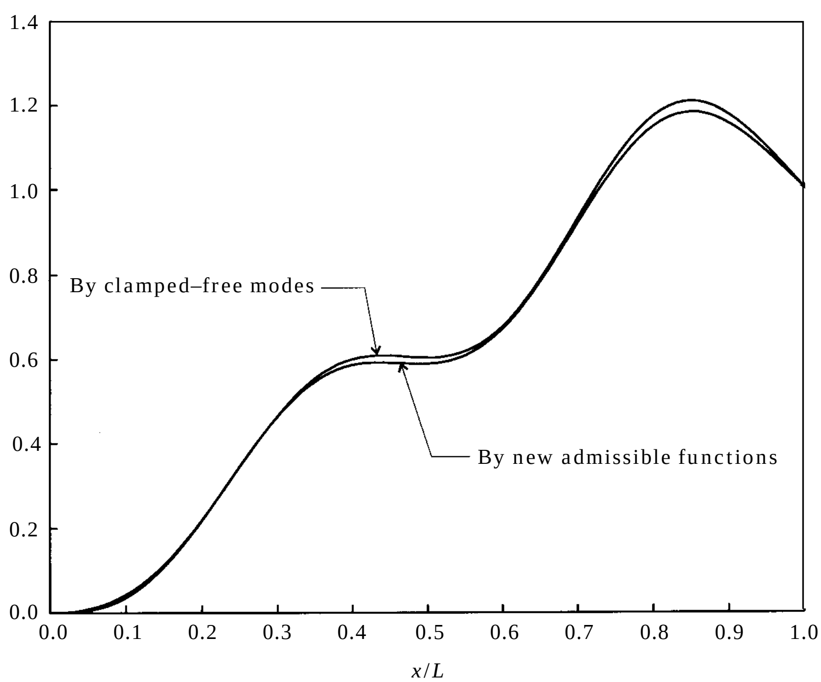

Figure 4. The fourth eigenvector.

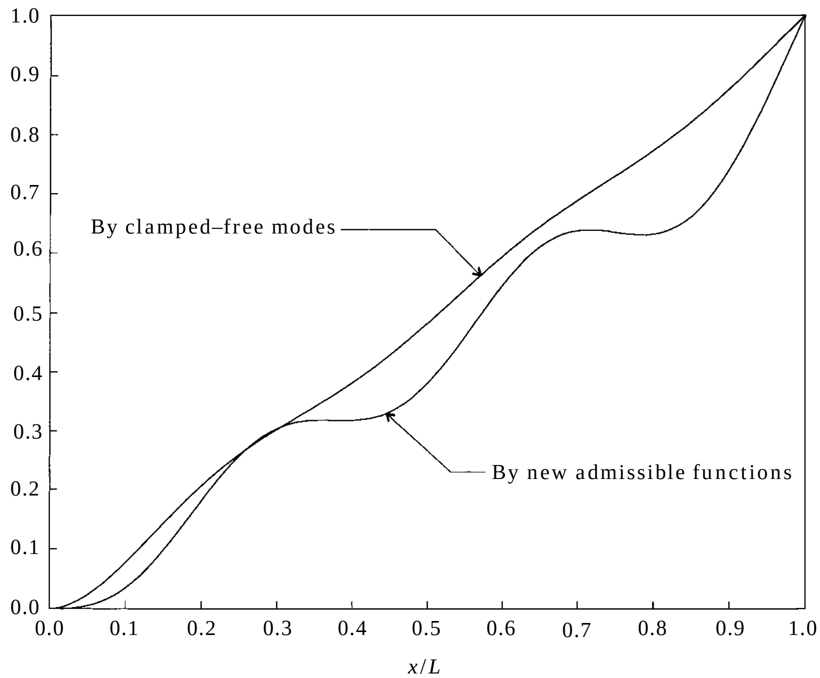

Figure 5. The fifth eigenvector.

frequencies by the new admissible function is faster than the one by the cantilever modes. The corresponding eigenvectors for the case of five admissible functions are as follows:

$$U_{cf}=\begin{bmatrix} 2\cdot267787 & 5\cdot973987 & 10\cdot450568 & 14\cdot779259 & 18\cdot824381 & -95\cdot476437 \\ 0\cdot000000 & -3\cdot003119 & -4\cdot111172 & -6\cdot356664 & -7\cdot731835 & 39\cdot922482 \\ 0\cdot000000 & 0\cdot595972 & -1\cdot590689 & -1\cdot119188 & -1\cdot983047 & 8\cdot759728 \\ 0\cdot000000 & 0\cdot013940 & 0\cdot747083 & -1\cdot065033 & -0\cdot419586 & 3\cdot248803 \\ 0\cdot000000 & 0\cdot003923 & 0\cdot031493 & 0\cdot824762 & -0\cdot884682 & 1\cdot560588 \\ 0\cdot000000 & 0\cdot000108 & 0\cdot014043 & 0\cdot050072 & 0\cdot904371 & 1\cdot355484 \end{bmatrix}, \tag{49}$$

$$U_{new}=\begin{bmatrix} 2\cdot267787 & 5\cdot975217 & 10\cdot435494 & 14\cdot883058 & 18\cdot949607 & -24\cdot004572 \\ 0\cdot000000 & -9\cdot282804 & 3\cdot056031 & -2\cdot105336 & 1\cdot465521 & 1\cdot062884 \\ 0\cdot000000 & -0\cdot011770 & -9\cdot719819 & 2\cdot812153 & -1\cdot934332 & -1\cdot353335 \\ 0\cdot000000 & -0\cdot043659 & 0\cdot131443 & -19\cdot697137 & 5\cdot157328 & 3\cdot472750 \\ 0\cdot000000 & 0\cdot009925 & -0\cdot125682 & 0\cdot313478 & -20\cdot061953 & -4\cdot817372 \\ 0\cdot000000 & -0\cdot005877 & 0\cdot053944 & -0\cdot294990 & 0\cdot609829 & 29\cdot794938 \end{bmatrix}. \tag{50}$$

The first column and row correspond to the rigid-body rotation. As can be seen from the above, the eigenvectors obtained by the clamped–free mode approximation depend heavily on the first assumed mode. On the other hand, the new set of assumed modes results in the diagonally dominant eigenvector matrix, which implies that new assumed

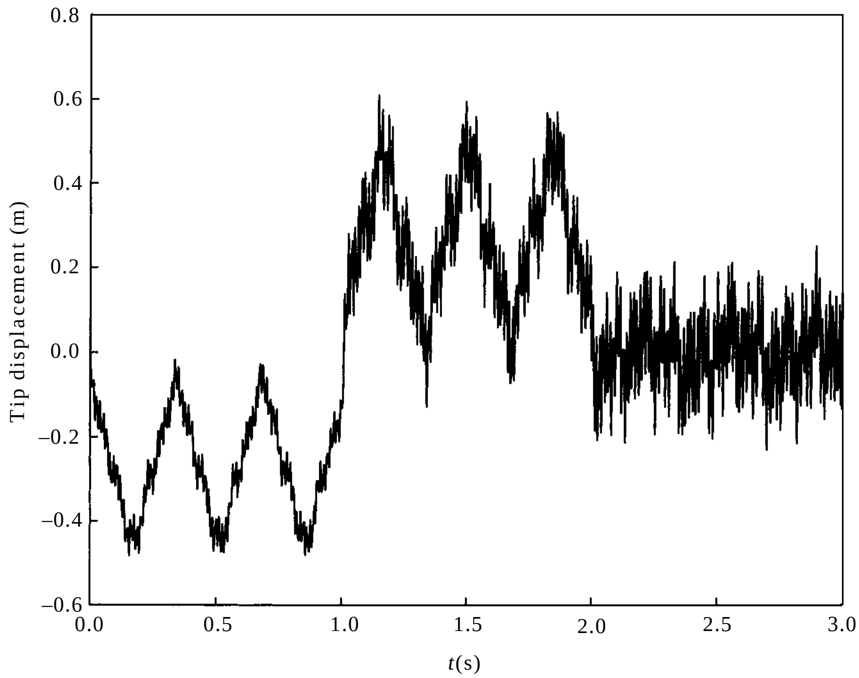

Figure 6. Tip displacement via clamped–free modes.

modes are closer to real mode shapes. Based on the above eigenvectors, the fourth and fifth mode shapes are plotted in Figures 4 and 5, from which it can be seen that the cantilever mode approximation suffers in the higher modes.

As a second numerical example, bang–bang torque is applied to the root of the beam.

$$\tau = \begin{cases} 1 & 0 \leqslant t \leqslant 2 \\ -1 & 2 < t \leqslant 4 \\ 0 & t > 4 \end{cases}. \tag{51}$$

The state equation, equation (43), is discretized with the sampling period of 0·01 s. Figures 6 and 7 show the time-history of the tip displacements by the cantilever modes and by the new admissible functions. It becomes evident that the new admissible functions give better simulation performance.

6. SUMMARY AND CONCLUSIONS

This paper is concerned with the modelling of a slewing beam by means of the assumed mode method. Interest lies in choosing proper assumed modes for better dynamic characteristics. It is generally known that discretization by any set of admissible functions is sufficient, provided that the set of functions is complete and a sufficiently large number of functions is taken. Although eigenfunctions of the non-rotating clamped–free uniform beam has been widely used as assumed modes for the dynamic analysis of the slewing beam, the numerical accuracy in the response calculation as well as natural frequencies and modes has never been pursued. The modelling issue becomes even more critical in numerical simulation since a large number of assumed modes results in a large-degree-of-freedom model, resulting in a numerically stiff equation. In this regard, the

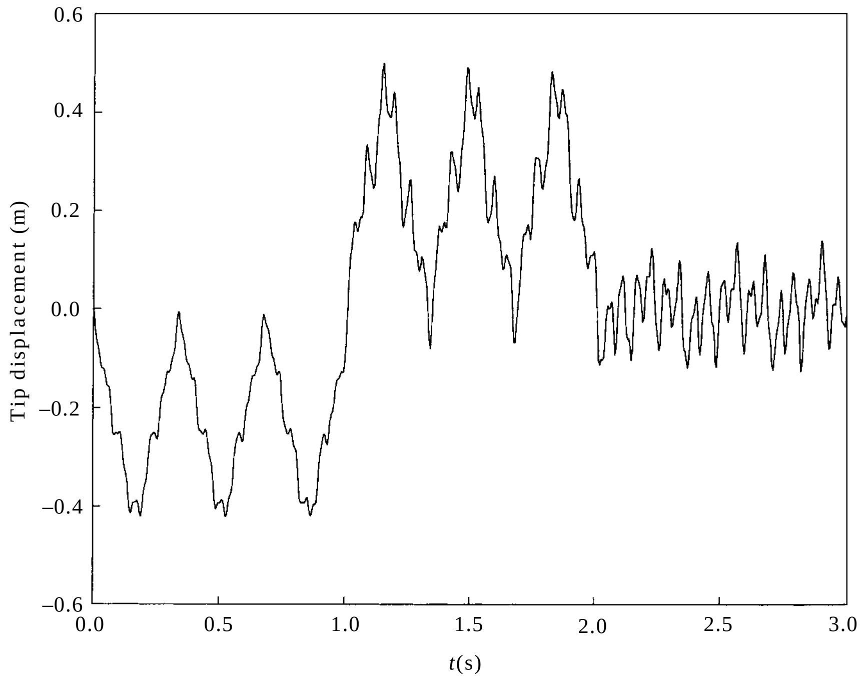

Figure 7. Tip displacement via new admissible functions.

system should be modelled accurately with a small number of assumed modes. To this end, the new set of admissible functions obtained for a slewing uniform beam is considered in this paper. The new set of assumed modes predicts natural frequencies and modes accurately, whereas eigenfunctions of the non-rotating clamped–free uniform beam suffer in higher modes. Numerical simulation results also show that eigenfunctions of the non-rotating clamped–free uniform beam suffer in simulating responses of the slewing beam since it does not field realistic higher modes. On the other hand, the new admissible functions developed in this paper give stable performance in numerical simulation.

REFERENCES

1. L. Meirovitch 1980 *Computational Method for Structural Dynamics*. Alphen aan der Rijn: Noordhoff Sitjhoff.
2. L. Meirovitch 1976 *AIAA Journal* **14**, 1387–1394. A stationary principle for the eigenvalue problem for rotating structures.
3. M. K. Kwak and L. Meirovitch 1992 *Journal of Guidance, Control, and Dynamics* **15**, 1342–1353. A new approach to the maneuvering and control of flexible multibody systems.
4. M. K. Kwak, K. K. Denoyer and D. Sciulli 1993 *Proceedings of the Ninth VPI&SU Symposium on Dynamics and Control of Large Structures, Blacksburg, VA*. Dynamics and control of a slewing active beam.
5. E. Garcia and D. J. Inman 1991 *Journal of Guidance, Control, and Dynamics* **14**, 736–742. Modeling of the slewing control of a flexible structure.
6. T. P. Mitchell and J. C. Bruch, Jr. 1989 *Journal of Guidance, Control, and Dynamics* **12**, 935–938. Dynamics of a rotationally accelerated beam.